Magnetic Properties of the Europium(III) Complex – Possible Multiplet Crossover

Romana Mičová, Zuzana Bielková, Cyril Rajnák, Ján Titiš, Ján Moncoľ, Alina Bienko, Roman Boča

---

Supplementary Information

Chemicals and handling

All chemicals were purchased and used as received. The solids (1,3-diamino-2-hydroxypropanole, 99 %, Acros Organics; 3-methoxysalicylaldehyde 99 %, Acros Organics; Europium(III) nitrate hexahydrate 99.9 %, Alfa Aesar; Zinc(III) nitrate hexahydrate 98 %, CentralChem) and solvents (ethanol 96 %; methanol p.a.) were used without any further purification. All manipulations were performed on air. The products were filtered over ashless paper.

Synthesis of H_3L

The Schiff base ligand (H_3L) was prepared as reported elsewhere [1,2].

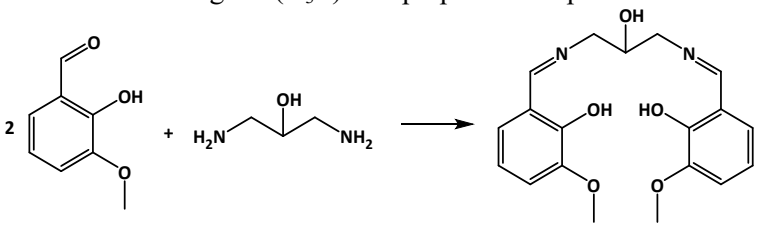

Scheme 1. Synthetic route for preparation of imine ligand H_3L.

1. Rajnák, C.; Dolai, M.; Alii, M.; Titiš, J.; Boča, R., Slow magnetic relaxation in Cu(II)-Eu(III) and Cu(II)-La(III) complexes. New. J. Chem. 2019, 43, 12698–12701. https://doi.org/10.1039/C9NJ02039J.
2. Dolai, M.; Mistri,T.; Panja,A.; Alia, M., Diversity in supramolecular self-assembly through hydrogen-bonding interactions of non-coordinated aliphatic –OH group in a series of heterodinuclear CuIIM (M = NaI, ZnII, HgII, SmIII, BiIII, PbII and CdII). Inorg. Chim. Acta 2013, 399, 95-104. https://doi.org/10.1016/j.ica.2013.01.006.

Properties. θ_f = 115-120°C. *Anal Calc.* (%) for $C_{19}H_{22}N_2O_5$ (M = 385.15 g·mol^{-1}): C, 63.86; H, 6.19; N, 7.82. Found: C, 63.19; H, 6.09; N, 7.83. **^{1}H NMR** (600 MHz, DMSO-d_6, 25 °C) δ (ppm) 13.75 (bs, OH, 2H), 8.51 (s, -CH=N-, 2H), 7.02 (d, J = 7.9 Hz, H-4', H-6', 4H), 6.78 (t, J = 7.8 Hz, H-5', 2H), 5.25 (d, J = 4.7 Hz, OH, 1H), 4.04-3.98 (m, H-2, 1H), 3.78 (s, OCH_3, 6H), 3.77 (ddd, J = 12.2, 4.4, 1.0 Hz, H-1, H-3, 2H), 3.60 (ddd, J = 12.3, 6.7, 0.7 Hz, H-1, H-3, 2H); **^{13}C NMR** (150 MHz, DMSO-d_6, 25 °C) δ (ppm) 167.2 (-CH=N-), 152.3 (C-2'), 148.2 (C-3'), 123.2 (C-6'), 118.3 (C-1'), 117.4 (C-5'), 114.7 (C-4'), 69.3 (C-2), 62.0 (C-1, C-3), 55.7 (OCH_3). **Selected IR bands** (cm^{-1}): 3485(w), 3306(w), 3016(w), 2948(w), 2903(w), 2835(w), 1634(s) for ν(C=N), 1521(m), 1471(s), 1456(sh), 1418(sh), 1371(w), 1334(sh), 1247(s), 1204(sh), 1168(w), 1120(m), 1077(s), 1051(m), 980(m), 950(m), 922(m), 834(m), 731(s), 605(m), 577(m), 513(m), 486(m). **UV-VIS** (EtOH) $\nu_{max}/10^3$ cm^{-1} (relat absorb.; e/M^{-1}·cm^{-1}) (c = 6.21·10^{-5} mol·dm^3): 23.98 (0.158; 2544), 30.21 (0.253; 40774), 33.88 (0.456; 7343), 37.92 (1.178; 18968), 45.01 (2.203; 35473).

Synthesis of $[(H_2O)Zn^{II}(LH)Eu^{III}(NO_3)_3]$ (1)

A 25 cm^3 methanol solution of $Zn(NO_3)_2{\cdot}6H_2O$ (0.297 g, 1.0 mmol) was added to a solution of H_3L (0.358 g, 1.0 mmol) containing triethylamine (TEA) (0.275 cm^3, 2.0 mmol) in methanol (30 cm^3) at room temperature under constant stirring. The resulting mixture is stirred for 10 min, and then finely powdered europium nitrate $Eu(NO_3)_3{\cdot}6H_2O$ (0.446 g, 1.0 mmol) was added. After being stirred for 1h, the mixture was filtered to remove the precipitate, if any. After a few days, yellow single crystals (needle-like), suitable for X-ray diffraction were precipitated out and collected by filtration. θ_f = 247-250°C. Yield: 0.557 g (72%). IR (cm^{-1}): 1619 for ν(C=N), 3134 for ν(alcoholic –OH); ν(nitrate) 1449s, 1322s. *Anal. calcd*. (%) for $C_{19}H_{22}EuN_5O_{15}Zn$, M_r = 777.76: C 29.34, H 2.85, N 9.00. Found: C 29.68, H 3.68, N 9.17.

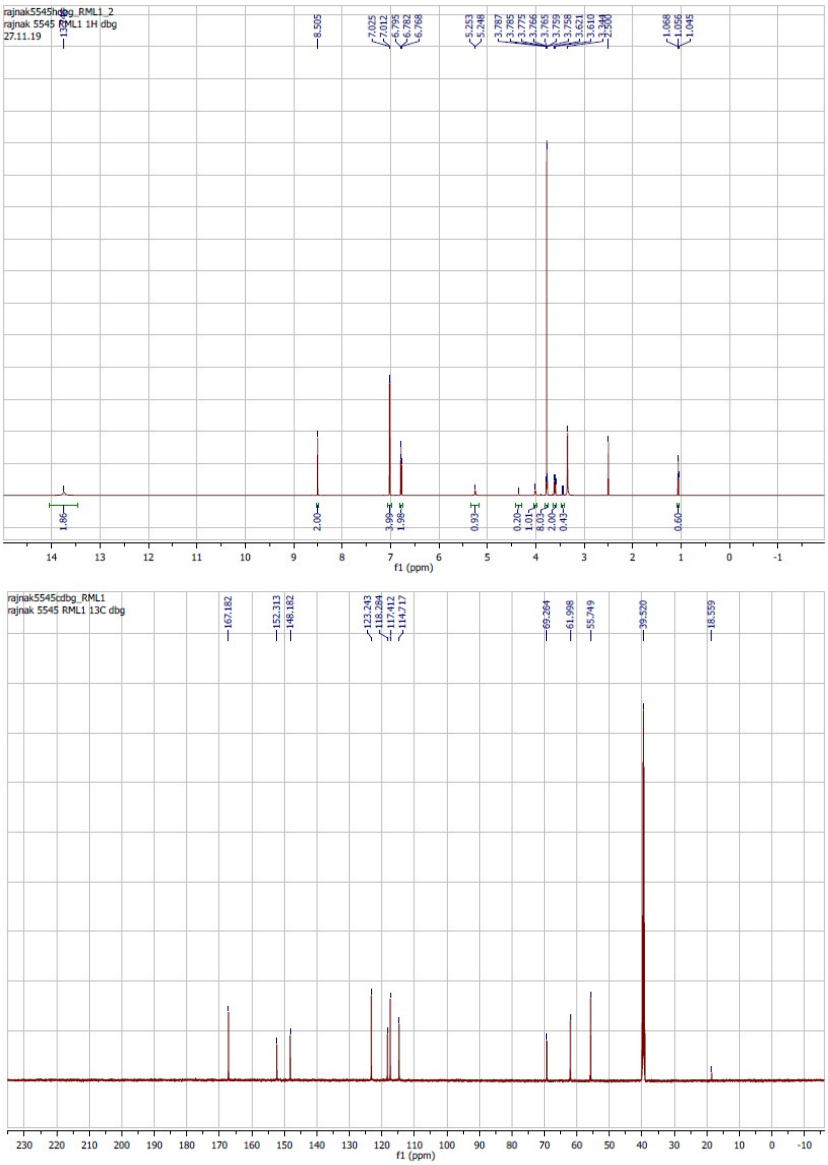

Figure S1. ^{1}H NMR spectrum of ligand H_3L (top) and ^{13}C NMR spectrum (bottom).

Table S1. Crystal data and structure determination

	$[(H_2O)Zn^{II}(LH)Eu^{III}(NO_3)_3]$ (**1**)
Empirical formula	$C_{19}H_{22}EuN_5O_{15}Zn$
Formula weight	777.74
Temperature/K	100.0
Crystal system	monoclinic
Space group	$P2_1/c$
a/Å	9.1308(6)
b/Å	28.357(3)
c/Å	10.3214(8)
α/°	90
β/°	105.792(6)
γ/°	90
Volume/Å^3	2571.6(4)
Z	4
ρ_{calc} g/cm^3	2.009
μ/mm-1	19.200
F(000)	1536.0
Crystal size/mm^3	0.28 × 0.03 × 0.01
Radiation	CuKα (λ = 1.54186)
2Θ range for data collection/°	9.436 to 133.206
Index ranges	-10 ≤ h ≤ 10, -33 ≤ k ≤ 31, -5 ≤ l ≤ 12
Reflections collected	16856
Independent reflections	4284 [Rint = 0.07171, Rsigma = 0.04544]
Data/restraints/parameters	4284/68/387
Goodness-of-fit on F^2	1.068
Final R indexes [I>=2σ (I)]	R1 = 0.0915, wR2 = 0.2616
Final R indexes [all data]	R1 = 0.1044, wR2 = 0.2735

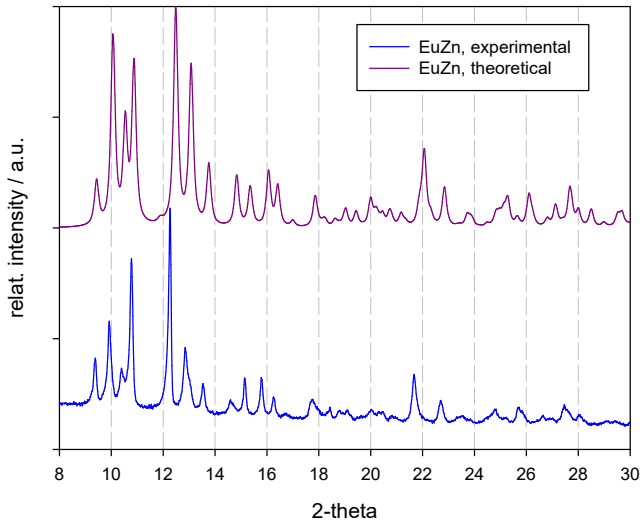

Figure S2. Calculated powder diffraction pattern for **1** from cif file (up) and recorded pattern using λ = 1.54060 Å (down).

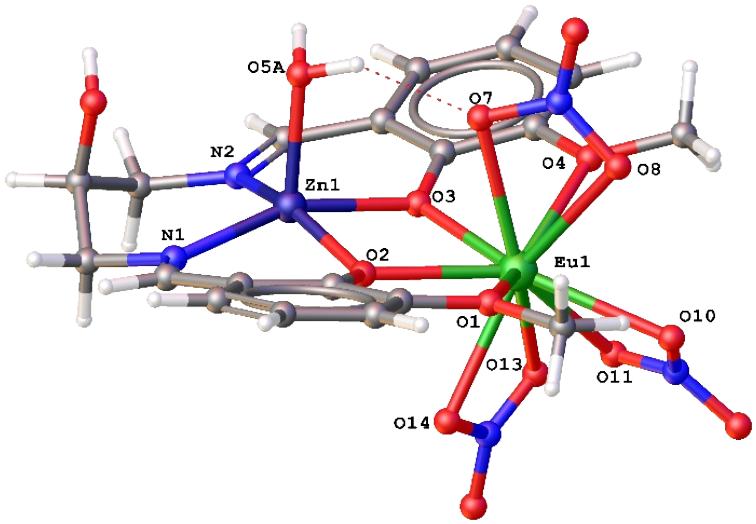

Figure S3. Molecular structure of 1 with atom labeling.

Table S2. Bond lengths (Å) and bond angles (deg) within the coordination polyhedra of **1**.

Eu1-O3	2.333(8)	Eu1-O9	2.503(10)	Zn1-O3	2.062(10)
Eu1-O2	2.336(9)	Eu1-O10	2.470(11)	Zn1-O2	2.016(9)
Eu1-O4	2.515(9)	Eu1-O7	2.515(17)	Zn1-O5	2.067(13)
Eu1-O1	2.526(8)	Eu1-O8	2.499(14)	Zn1-N2	2.058(11)
Eu1-O15	2.509(17)	Eu1-O7A	2.53(2)	Zn1-N1	2.050(12)
Eu1-O14	2.672(14)	Eu1-O8A	2.52(2)		
O1-Eu1-O4	146.0(3)	O2-Eu1-O4	127.4(3)	O4-Eu1-O7A	86.3(4)
O2-Eu1-O3	64.8(3)	O1-Eu1-O2	65.4(3)	O4-Eu1-O8A	72.7(6)
O1-Eu1-O3	125.9(3)	O2-Eu1-O15	150.8(4)	O1-Eu1-O7A	100.6(6)
O1-Eu1-O14	66.3(4)	O2-Eu1-O14	125.2(4)	O4-Eu1-O15	71.0(3)
O3-Eu1-O15	119.9(4)	O2-Eu1-O9	75.4(3)	O1-Eu1-O15	113.8(3)
O3-Eu1-O14	167.6(4)	O2-Eu1-O10	119.6(4)	O7A-Eu1-O15	86.1(7)
O3-Eu1-O9	73.1(3)	O2-Eu1-O7	87.5(4)	O8A-Eu1-O15	46.8(6)
O3-Eu1-O10	113.0(3)	O2-Eu1-O8	78.3(4)	O4-Eu1-O9	78.5(3)
O3-Eu1-O7	69.3(4)	O2-Eu1-O7A	66.3(6)	O1-Eu1-O9	75.2(3)
O3-Eu1-O8	109.6(4)	O2-Eu1-O8A	111.9(6)	O9-Eu1-O15	133.6(4)
O3-Eu1-O7A	77.6(7)	O4-Eu1-O14	107.2(3)	O9-Eu1-O14	115.0(4)
O3-Eu1-O8A	82.0(7)	O4-Eu1-O7	86.3(4)	O7-Eu1-O9	142.4(4)
O14-Eu1-O15	47.7(4)	O7-Eu1-O15	70.0(5)	O7A-Eu1-O9	139.0(7)
O8A-Eu1-O9	148.1(7)	O4-Eu1-O10	71.2(3)	O1-Eu1-O10	75.5(3)
O10-Eu1-O15	86.3(4)	O10-Eu1-O14	69.9(4)	O9-Eu1-O10	50.5(3)
O7-Eu1-O10	151.7(5)	O8-Eu1-O10	137.3(4)	O7A-Eu1-O10	169.1(7)
O8A-Eu1-O10	128.0(6)	O1-Eu1-O7	127.5(4)	O7-Eu1-O14	102.2(4)
O4-Eu1-O8	131.3(4)	O1-Eu1-O8	79.3(4)	O8-Eu1-O15	73.1(4)
O8-Eu1-O14	68.6(4)	O8-Eu1-O9	149.1(4)	O7-Eu1-O8	50.5(4)
O7A-Eu1-O14	99.2(7)	O1-Eu1-O8A	136.6(6)	O8A-Eu1-O14	86.9(7)
O3-Zn1-Eu1	38.1(2)	O2-Zn1-Eu1	37.8(3)	O5-Zn1-Eu1	97.0(4)
N2-Zn-Eu1	124.7(3)	N1-Zn1-Eu1	126.1(3)	Zn1-O3-Eu1	108.8(4)
Zn1-O2-Eu1	110.3(4)	O2-Zn1-O3	75.7(4)	O2-Zn1-O5	96.6(5)
O2-Zn1-N2	154.4(4)	O2-Zn1-N1	89.4(4)	N2-Zn1-O3	88.0(4)
N2-Zn1-O5	105.5(5)	N1-Zn1-O3	157.4(4)	N1-Zn1-O5	99.4(5)
N1-Zn1-N2	99.4(5)				

Table S3. SHAPE analysis of the coordination polyhedra

Central atom	Coord. number	Chromophore	Agreement index	Geometry
Zn	5	$\{ZnO_3N_2\}$	1.253	4py
Eu	10	$\{EuO_9\}$	4.271	bc4a

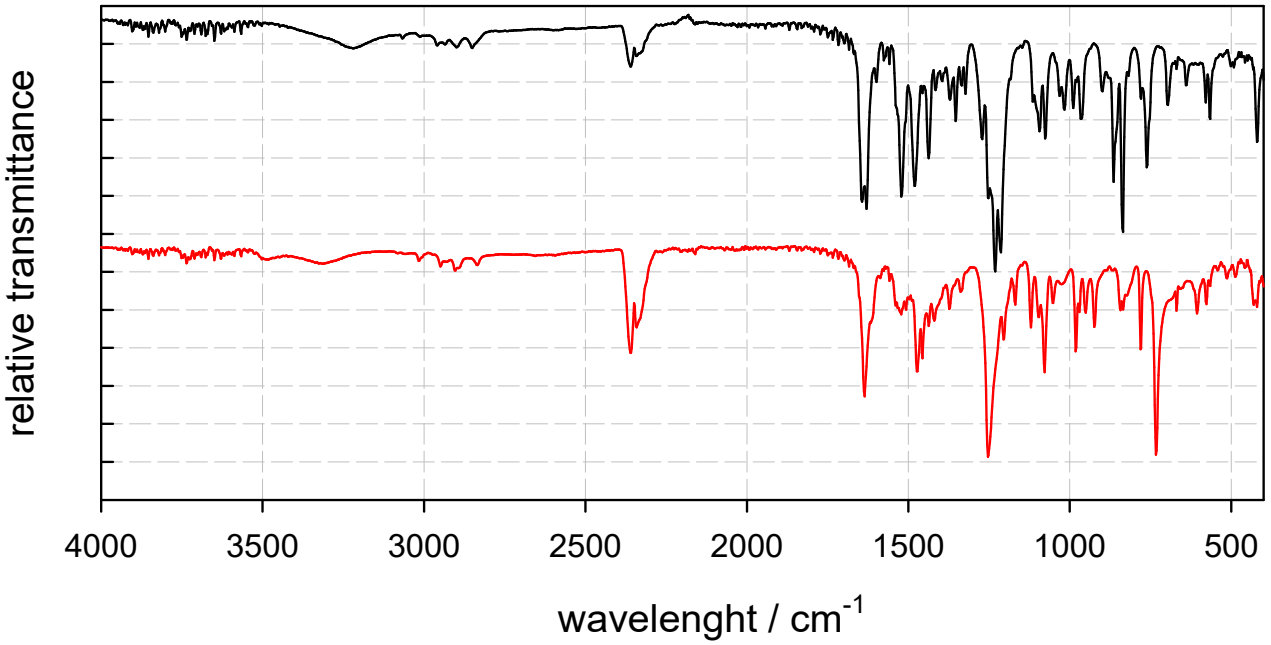

Figure S4. FT-IR (ATR) spectrum of H_3L (red, bottom) and **1** (black, top).

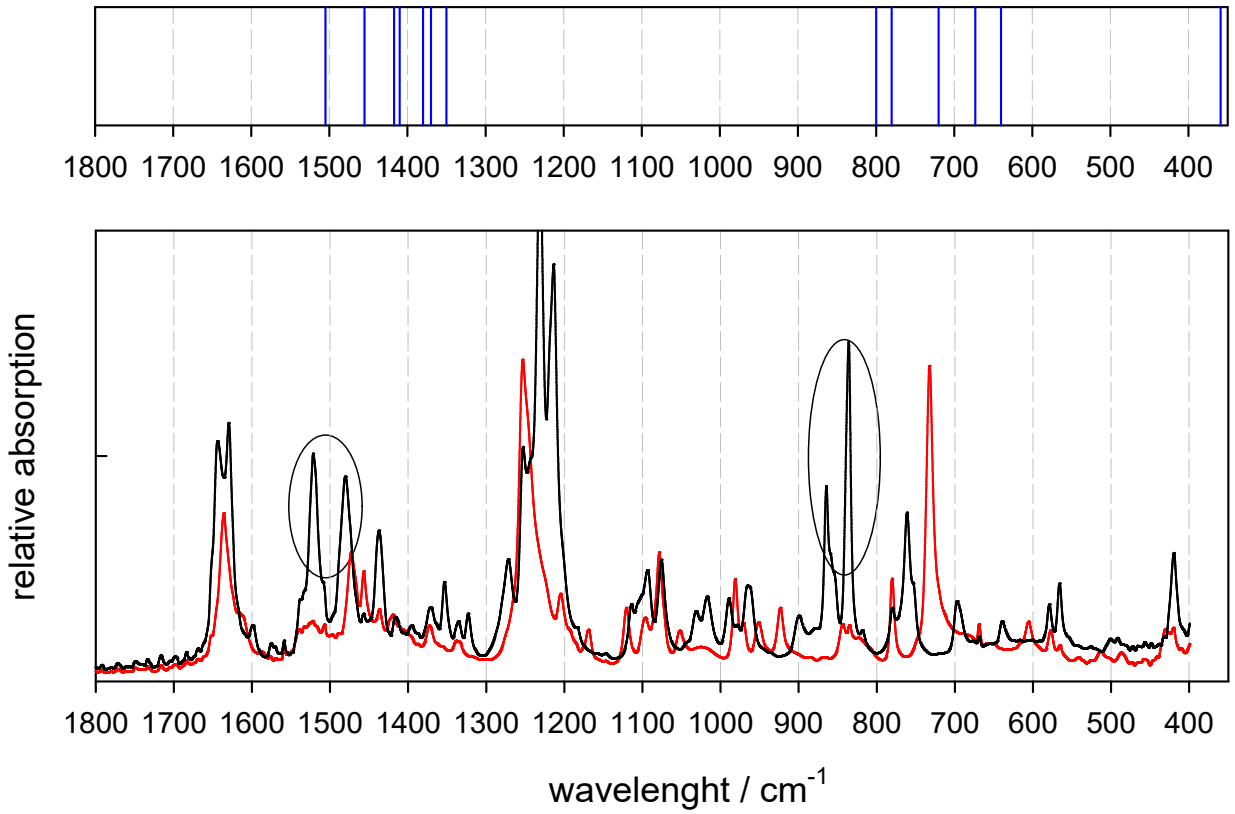

Figure S5. Low-frequency IR spectrum of H_3L (red) and **1** (black) in the absorbance mode along with calculated transitions (vertical bars). Additional peaks at ca 850 and 1500 cm^{-1} might correspond to the direct $^7F_0 \rightarrow {}^7F_2$ and $^7F_0 \rightarrow {}^7F_3$ transitions.

Table S4. SOC corrected absorption spectrum (SA-CASSCF+SOMF).

States	Energy (cm-1)	Wavelength (nm)	fosc	T2 (D**2)	|TX| (D)	|TY| (D)	|TZ| (D)
$^7F_0$ → $^7F_1$							
0 1	132.1	75676.8	0.000000000	0.00000	0.00001	0.00001	0.00000
0 2	248.7	40202.5	0.000000000	0.00000	0.00003	0.00006	0.00002
0 3	359.2	27839.7	0.000000000	0.00000	0.00009	0.00008	0.00019
$^7F_0$ → $^7F_2$							
0 4	641.8	15581.6	0.000000000	0.00000	0.00045	0.00023	0.00119
0 5	673.0	14858.6	0.000000001	0.00000	0.00097	0.00092	0.00175
0 6	718.9	13909.5	0.000000000	0.00000	0.00024	0.00075	0.00062
0 7	780.8	12808.1	0.000000000	0.00000	0.00059	0.00029	0.00100
0 8	798.1	12530.4	0.000000001	0.00001	0.00110	0.00248	0.00076
$^7F_0$ → $^7F_3$							
0 9	1357.7	7365.6	0.000000000	0.00000	0.00022	0.00044	0.00002
0 10	1370.2	7298.3	0.000000000	0.00000	0.00004	0.00009	0.00018
0 11	1386.6	7211.7	0.000000000	0.00000	0.00032	0.00008	0.00022
0 12	1411.0	7087.3	0.000000000	0.00000	0.00006	0.00046	0.00018
0 13	1417.5	7054.5	0.000000000	0.00000	0.00003	0.00015	0.00021
0 14	1455.9	6868.7	0.000000000	0.00000	0.00040	0.00080	0.00043
0 15	1503.9	6649.5	0.000000000	0.00000	0.00013	0.00006	0.00001

Table S5. *Ab initio* (SA-CASSCF+SOMF) calculated energies of the multiplets $^7F_0$ through $^7F_6$

Eigenvalues		cm^{-1}	eV	Boltzmann populations at T = 300K
7F0	0:	0.00	0.0000	4.58e-01
3 multiplets				
7F1	1:	132.14	0.0164	2.43e-01
7F1	2:	248.74	0.0308	1.39e-01
7F1	3:	359.20	0.0445	8.18e-02
5 multiplets				
7F2	4:	641.78	0.0796	2.11e-02
7F2	5:	673.01	0.0834	1.82e-02
7F2	6:	718.93	0.0891	1.46e-02
7F2	7:	780.76	0.0968	1.08e-02
7F2	8:	798.06	0.0989	9.97e-03
7 multiplets				
7F3	9:	1357.67	0.1683	6.81e-04
7F3	10:	1370.19	0.1699	6.41e-04
7F3	11:	1386.63	0.1719	5.92e-04
7F3	12:	1410.97	0.1749	5.27e-04
7F3	13:	1417.53	0.1758	5.11e-04
7F3	14:	1455.88	0.1805	4.25e-04
7F3	15:	1503.87	0.1865	3.38e-04
9 multiplets				
7F4	16:	2202.98	0.2731	1.18e-05
7F4	17:	2235.50	0.2772	1.01e-05
7F4	18:	2253.42	0.2794	9.27e-06
7F4	19:	2310.15	0.2864	7.07e-06
7F4	20:	2398.58	0.2974	4.62e-06
7F4	21:	2402.68	0.2979	4.53e-06
7F4	22:	2421.20	0.3002	4.15e-06
7F4	23:	2465.42	0.3057	3.36e-06
7F4	24:	2473.86	0.3067	3.22e-06
11 multiplets				
7F5	25:	3365.82	0.4173	4.47e-08
7F5	26:	3393.84	0.4208	3.91e-08
7F5	27:	3454.47	0.4283	2.92e-08
7F5	28:	3455.47	0.4284	2.91e-08
7F5	29:	3497.61	0.4336	2.38e-08
7F5	30:	3539.04	0.4388	1.95e-08
7F5	31:	3555.71	0.4409	1.80e-08
7F5	32:	3597.49	0.4460	1.47e-08
7F5	33:	3612.52	0.4479	1.37e-08
7F5	34:	3640.59	0.4514	1.20e-08
7F5	35:	3648.62	0.4524	1.15e-08
13 multiplets:				
7F6	36:	4716.89	0.5848	6.86e-11
7F6	37:	4717.52	0.5849	6.84e-11
7F6	38:	4805.13	0.5958	4.49e-11
7F6	39:	4814.84	0.5970	4.29e-11
7F6	40:	4851.99	0.6016	3.59e-11
7F6	41:	4887.77	0.6060	3.02e-11
7F6	42:	4903.82	0.6080	2.80e-11
7F6	43:	4956.08	0.6145	2.18e-11
7F6	44:	4959.67	0.6149	2.14e-11
7F6	45:	5020.28	0.6224	1.60e-11
7F6	46:	5021.41	0.6226	1.59e-11
7F6	47:	5101.35	0.6325	1.09e-11
7F6	48:	5101.52	0.6325	1.08e-11

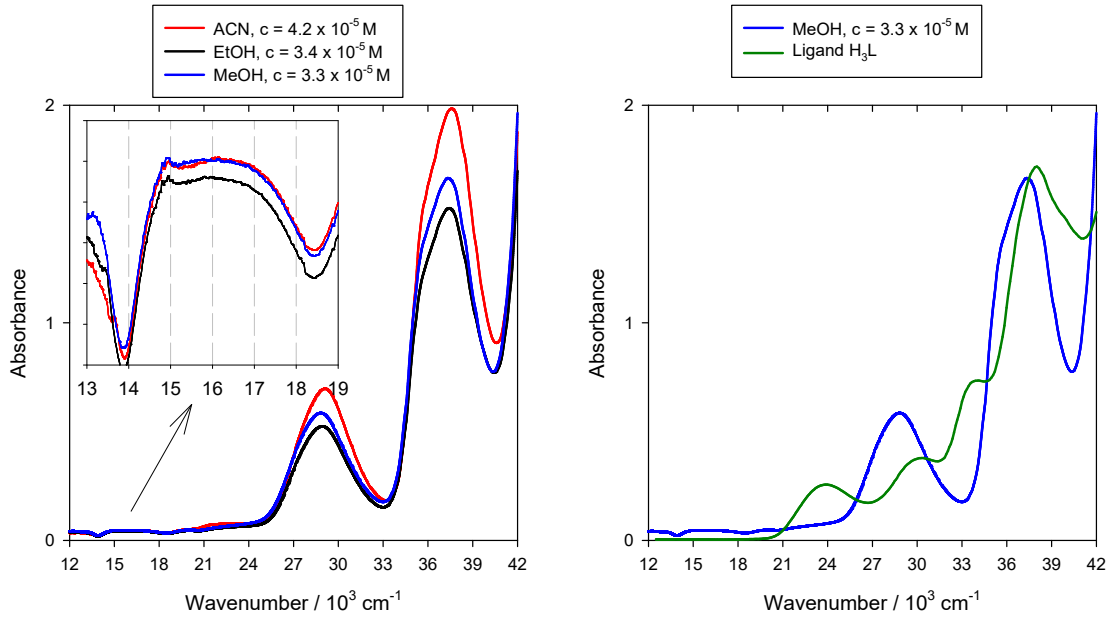

Figure S6. Electronic UV/Vis spectra of **1** in various solvents.

DC magnetization

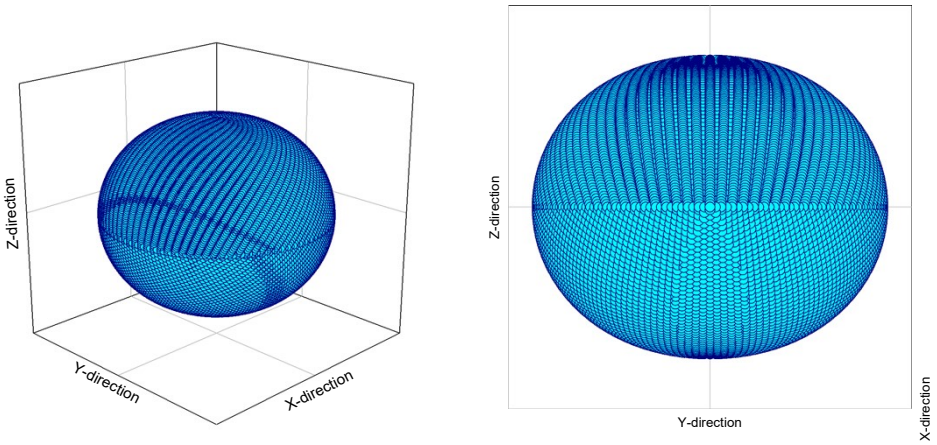

Figure S7. 3D view of the magnetization at T = 2.0 K and B = 1.0 T calculated from the fitted magnetic parameters for **1** (see main text). Result – slight easy plane (z-compression).

AC susceptibility data

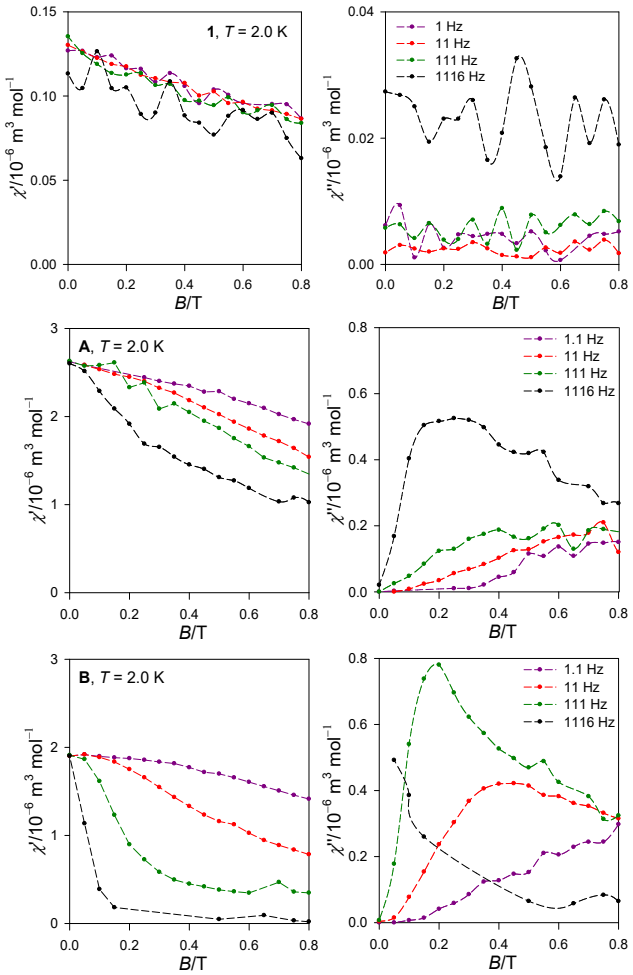

Figure S8. AC susceptibility data for $[(H_2O)Zn^{II}(LH)Eu^{III}(NO_3)_3]$ (**1**) $[(H_2O)Cu^{II}(LH)Eu^{III}(NO_3)_3]$ (**A**) and $[(H_2O)Cu^{II}(LH)La^{III}(NO_3)_3]$ (**B**). Note: the AC response for **1** is ca 20-times lower relative to **A** and close to the detection limit of the MPMS apparatus (magnetic moment m" ~ 10^{-8} - 10^{-7} emu).

A multiplet crossover

In interpreting the experimental susceptibility data an alternate view has been applied – a two level model. Basically, it has roots in theory of the spin crossover that is well elaborated. The ground levels (low in energy, L) is diamagnetic ($J_L = 0$), however possessing some temperature independent paramagnetism originating in the admixture of the excited magnetic state via spin-orbit interaction. This works like the van Vleck term α_L. The excited level (high in energy, H) is magnetic ($J_H = 1$) and obeying the Curie law with g_H

$$\chi = (1 - x_H)\alpha_L + x_H \frac{N_A \mu_0 \mu_B^2}{3 k_B T} g_H^2 J_H (J_H + 1)$$

The separation between them is Δ_0. Then the regular solution model of the spin crossover, equivalent to the two-level Ising-like model,[20] offers an expression for the mole fraction of the high-energy state $0 < x_H < 1$ in the form

$$x_H = (1 + \sigma)/2$$

obeying the implicit equation

$$\sigma = \frac{r_{eff} \exp[-(\Delta_0 - 2\gamma\sigma)/k_B T] - 1}{r_{eff} \exp[-(\Delta_0 - 2\gamma\sigma)/k_B T] + 1}$$

where the effective degeneracy ratio involves the electronic and vibrational parts and $r_{eff} > 3$ is required for $J_H = 1$. Then the entropy and enthalpy of the transition are $\Delta S = R \ln r_{eff}$ and $\Delta H = N_A \Delta_0$, respectively. The susceptibility data was fitted with the above model yielding $\alpha_L = 72(1) \times 10^{-9}$ m^3 mol^{-1}, $g_H = 1.40(20)$, $\Delta_0 = 503(40)$ K = 350 cm^{-1}, and $r_{eff} = 3$ was fixed (the solid-state cooperativeness γ was omitted). The quality of the fit is perfect (Figure 3 in the main text). Notice, g_H is close to the theoretical prediction $g_H = 1.5$ for Eu(III) and independently fitted Δ_0 is close to λ(Eu). Derived thermodynamic parameters of the „multiplet crossover" are $\Delta H = 4.19$ kJ mol^{-1} and $\Delta S = 9.13$ J K^{-1} mol^{-1}. The transition temperature of the entropy driven process, when $x_H = 0.5$, is $T_{1/2} = \Delta H/\Delta S = 458$ K, and the equilibrium constant is $K = x_H/(1 - x_H)$.

(20) Boča, R.; Linert, W. Is There a Need for New Models of the Spin Crossover? *Monatsh. Chem*. **2003**, *134*, 199–216. DOI 10.1007/s00706-002-0489-4.